ACS Macro Letters

Letter

pubs.acs.org/macroletters

Enhanced Carbon Dioxide Adsorption by a Mesoporous Poly(ionic liquid)

Antje Wilke, Jiayin Yuan,* Markus Antonietti, and Jens Weber*

Max Planck Institute of Colloids and Interfaces, Colloid Chemistry, Science Park Golm, 14424 Potsdam, Germany

Supporting Information

ABSTRACT: The synthesis of a mesoporous poly(ionic liquid) network via a hard-templating pathway is presented. Structure analysis was carried out using gas adsorption, small-angle X-ray scattering, and electron microscopy. The mesoporous poly(ionic liquid) showed a significantly faster CO_2 adsorption than its nonporous counterpart. We found the adsorption is accompanied by strong interactions, which are also reflected in a high CO_2 over N_2 selectivity.

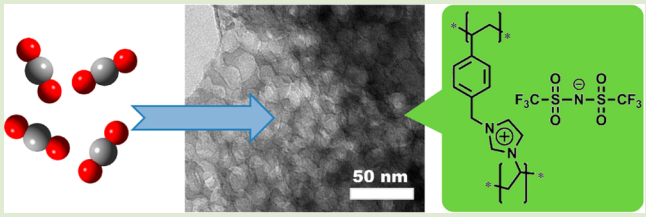

Poly(ionic liquid)s (PILs) stand for a subclass of polyelectrolytes, the repeating unit of which has ionic liquid (IL) character. The research scope in PILs recently has significantly expanded.[1] It is generally accepted that the incorporation of IL moieties into the polymer chain combines some of the unique characters of ILs with the common features of polymers. The synergistic effect produces immediately a variety of new (multi)functional materials,[1−4] among which the controlled capture or separation of carbon dioxide (CO_2) is of special interest. Several groups have reported that bulk PILs exhibited quick and enhanced CO_2 uptake compared to their low molecular IL counterparts. These research efforts were devoted mainly to PILs with novel chemical structure that showed a higher affinity to CO_2.

An orthogonal pathway is to provide PILs with a nanostructure with enlarged surface area to amplify the gas uptake. PIL nanoparticles have been reported recently, yet as colloids in aqueous solution.[5] There are a few reports on macroporous PILs,[5b,6] with surface areas of up to 37 $m^2 \cdot g^{-1}$.[6a] A mesoporous material (with pore sizes between 2 and 50 nm) would indeed provide on the one hand sufficiently high surface area and acceptable mass transfer at the same time. This explains the huge interest of the scientific community in mesoporous materials.[7]

Given the huge potential of PILs in gas sorption and separation but also heterogeneous catalysis, mesoporous PILs (mpPILs) are a next step to improve their functional properties. Herein we describe the synthesis of mpPILs via a hard-templating pathway, which feature well-defined mesopore sizes and pore shapes. The interactions and adsorption kinetics of the mpPILs with CO_2 are studied in detail.

The synthesis is based on hard-templating of silica nanoparticles.[8] Silica nanoparticles (LUDOX TM-50, nominal diameter: 25 nm) were slowly dried, forming thereby a mesoporous, opal-like silica. Backfilling of the interstitial voids with the monomer/initiator mixture and subsequent polymerization results in an organic−inorganic hybrid. Etching of the inorganic component finally liberates the mesoporous polymer (Scheme 1b). We learned from previous works that a high degree of cross-linking is necessary to stabilize the polymer structure against collapse after silica template removal.[9]

Scheme 1. (a) Synthetic Pathway towards the mpPIL and (b) Schematic Overview of the Employed Hard-Templating Pathway

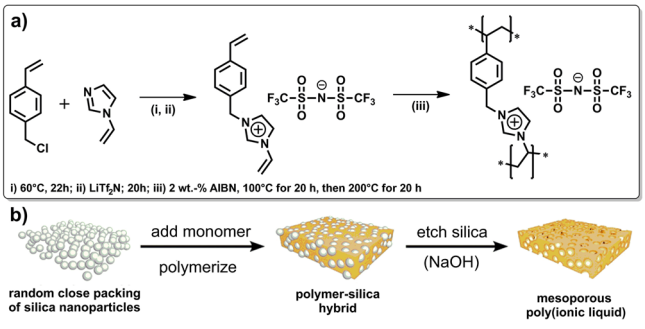

A cross-linkable monomer was prepared by reaction of 1-vinylimidazole with 4-vinyl benzyl chloride to yield 3-(4-vinylbenzyl)-1-vinylimidazolium chloride (Scheme 1a). The [Cl^-] anion was exchanged to bis(trifluoro methylsulfonyl)-imide [Tf_2N^-] to afford the room temperature IL state of the monomer. The polymerization was initiated after complete infiltration by heating to 100 °C for 20 h. Final curing at 200 °C for another 20 h produced transparent and amber-like PIL-silica hybrids. Etching of the silica was performed by treatment with 1 M NaOH, followed by neutralization, washing, and vacuum drying. Thermogravimetric analysis proved the complete removal of silica. A comparison of the Fourier transform infrared (FTIR) spectra of the IL monomer and the

Received: June 29, 2012
Accepted: July 24, 2012
Published: July 30, 2012

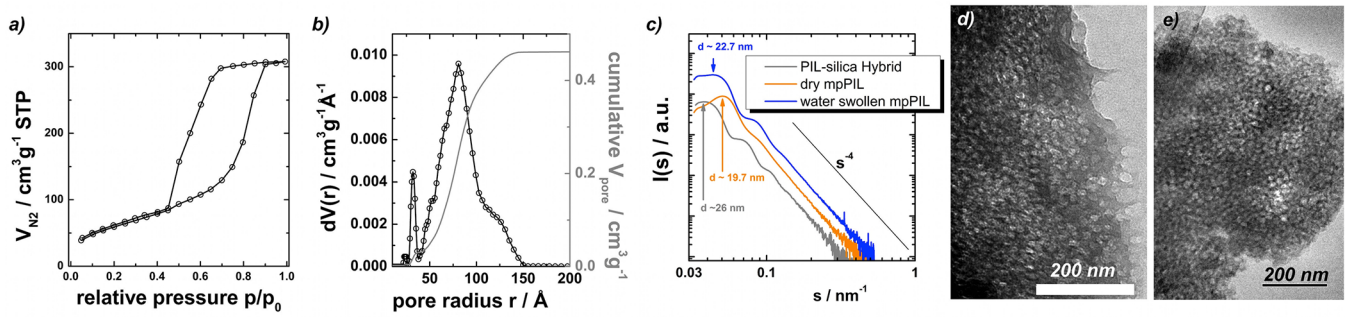

Figure 1. (a) N_2 adsorption/desorption isotherm of mpPIL measured at 77.3 K; (b) pore size distribution (black circles) and cumulative pore volume (gray line) of mpPIL calculated by QSDFT methodology using a spherical pore model (adsorption branch); (c) SAXS patterns of the PIL-silica hybrid (gray), the dry mpPIL (orange), and water-swollen mpPIL (blue); (d) TEM micrograph of mpPIL, scale bar: 200 nm; (e) Cryo-TEM of mpPIL, scale bar: 200 nm, image after background subtraction.

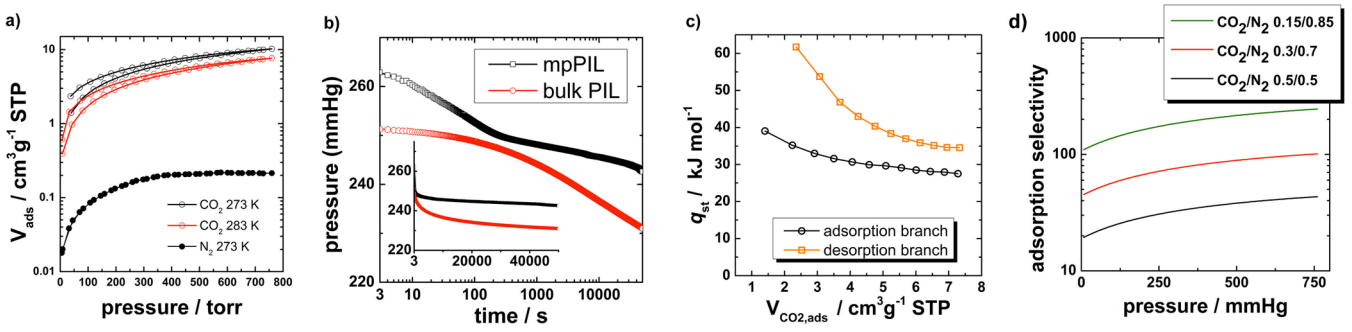

Figure 2. (a) CO_2 (open circles) and N_2 (closed circles) adsorption/desorption isotherms measured at 273 K and 283 K, respectively; (b) adsorption kinetics of the CO_2 adsorption in mpPIL and bulk PIL (inset: linear time scale); (c) isosteric heats of sorption calculated from the adsorption branch (black circles) and desorption branch (orange circles) of the CO_2 isotherms obtained at 273 and 283 K; (d) IAST prediction of the CO_2 over N_2 selectivity for different gas compositions (based on adsorption).

mpPIL proved clearly that the molecular structure survived the thermal polymerization and the silica etching (see the Supporting Information). The main difference is the vinyl band, which largely reduced in the mpPIL spectrum.

Strong vibration bands at 1200−1500 cm^{-1} are characteristic of $[Tf_2N^-]$, indicating that the $[Tf_2N^-]$ anion remained. This statement is strongly supported by elemental analysis, which showed a reasonable content of sulfur. Hence, we suggest that the mpPIL keeps the $[Tf_2N^-]$ during the fabrication, probably because of the high hydrophobicity introduced by the $[Tf_2N^-]$ ion.[6d,10] Nevertheless, partial exchange with external anions might occur at the interface.

The mesostructure of the mpPIL was analyzed by means of gas adsorption/desorption measurements, small-angle X-ray scattering (SAXS), and transmission electron microscopy (TEM and Cryo-TEM). N_2 adsorption gives initial access to the average pore size, porosity, and specific surface area. Specific surface areas ranging typically between 150 and 220 $m^2 \cdot g^{-1}$ were obtained applying the Brunauer−Emmett−Teller (BET) theory. Typical pore volumes are in the range of ∼0.45 $cm^3 \cdot g^{-1}$, which corresponds to a porosity of roughly 37% (ρ_{PIL} ∼ 1.3 $g \cdot cm^{-3}$). This is less than the volume filling of the silica particles within the template (∼69%), which points to volume shrinkage of the pores by a factor of 2.

The pore size distribution was calculated based on the quenched solid density functional theory (QSDFT) assuming spherical pores and a carbon-like adsorbent character.[11] The main fraction of pores was within the mesopore regime. We found that the maximum was situated at 15 nm, that is, 10 nm smaller than the used template, slightly overexpressing the expected pore shrinkage. A shoulder exists at a diameter of ∼25 nm, which is the mesopore size expected from the size of the template particles.

The SAXS pattern of the hybrid material, the dry mpPIL, and the water-swollen mpPIL are depicted in Figure 1c. The SAXS pattern of the hybrid material is identical to that of the silica template; that is, the polymerization within the interstitial voids does not affect the morphology. A Bragg peak can be identified at a *d*-spacing of ∼26 nm, which is due to the short-range order of the spherical particles (Percus−Yevick like).[12] At larger scattering vector *s*, the typical undulations of the form factor of spherical particles and the associated Porod decay (s^{-4}) are clearly visible. Upon drying, the pattern changes, and the maximum is shifted to smaller *d*-spacings of ∼19.7 nm. This, and the less defined scattering pattern, goes well with the macroscopically observed overall pore shrinkage and deformation as a consequence of the high interfacial energy which arises upon pore emptying. TEM micrographs of the dry materials do clearly show deformed pores as the majority component (Figure 1d), which seem to adopt an ellipsoidal shape. This is also in line with the observation of smaller pores by N_2 sorption as the semiminor axis (with length *L* and $L < R_{sphere}$) will dictate the condensation within the mesopores.

The mesopore collapse/deformation is reversible upon backfilling with solvent, that is, by reducing the interfacial forces, which is in line with previous reports.[13] The SAXS pattern of water-filled mpPIL (Figure 1c) does clearly reproduce the shape of the original hybrid material, indicating that the pores readopt a spherical shape. This is confirmed by cryo-TEM investigations, which show regularly shaped

dx.doi.org/10.1021/mz3003352 | ACS Macro Lett. 2012, 1, 1028−1031

spherical pores (Figure 2e and Figures S3−S4 of the Supporting Information).

PILs have been discussed as powerful carbon dioxide adsorbents for some time.[14] Usually, it is found that polymerized ILs show a higher CO_2 uptake compared to their monomer analogues. We were interested whether the presence of a pronounced specific surface area can increase the uptake capacity and kinetics even more. For that, we compared first the CO_2 uptake of the IL monomer used here, the bulk PIL, and the mesoporous PIL at 273 K and 760 mmHg. We found the highest uptake for mpPIL (~0.46 mmol·g^{-1}), with a lower uptake for the bulk PIL (~0.13 mmol·g^{-1}) and the monomeric species (~0.02 mmol·g^{-1}). Typically, all samples showed a hysteresis upon desorption; in the case of mpPIL, the hysteresis was however less pronounced. It is interesting to analyze whether this hysteresis is related to kinetic effects, strong binding events, or a mixture of both. To check this, the equilibrium settings of the gas adsorption machine were changed toward larger equilibration times. No significant change of the adsorption capacity was observed for mpPIL; that is, the measured isotherm is at least very close to equilibrium. The origin of the observed weak hysteresis might therefore indeed be due to CO_2−PIL interactions. Contrarily, the adsorption capacity of the bulk PIL increased depending on the time given for equilibration by up to a factor of 2 (Figure S5 of the Supporting Information).

We made an attempt to analyze the adsorption kinetics following a protocol developed by Smarsly et al.[15] (see Figure 2b). Carbon dioxide was expanded in the sample cell of the adsorption apparatus, and the change in pressure was monitored with time. Adsorption into the bulk PIL is obviously much slower than into the mesostructured PIL. This is illustrated by the ongoing significant adsorption into the bulk even after 30 h, while the major adsorption event into the mpPIL takes place within the first 5 min, in line with the equilibration experiment.

The interaction strength is typically accessed via the isosteric heat of adsorption (q_{st}). The adsorption isotherm of CO_2 on mpPIL at 283 K resembles the one measured at 273 K, with lower uptake. Calculation of q_{st} is possible but may be somewhat hampered due to the weak hysteresis. Using the adsorption branches of the isotherms, q_{st} is found to be in the range of 40−30 kJ·mol^{-1}, which is significantly higher than in, for example, activated carbon.[16] Performing the calculation using the desorption branches yields even higher values of q_{st}. This indicates that the hysteresis is potentially due to binding of CO_2 and a follow-up structural readjustment of the polymeric ionic liquids toward a higher energy adsorption situation; that is, the CO_2 "improves" its bed. The energies at the desorption site consequently contain an "activated structural relaxation part", which makes a direct assignment to the elemental desorption process difficult. However, it is clear from Figure 2c that the very high-energy differences are only found for the first molecules to adsorb, that is, the high energy adsorption sites.

For further elucidation of this effect, we also measured the N_2 uptake at 273 K and 760 mmHg, which allow for the calculation of the apparent single-gas selectivity of the gas pair CO_2/N_2 using the ideal adsorbed solution theory (IAST).[17] A high selectivity of ~45 was found for a 50:50 (v/v) mixture of CO_2 and N_2 at 273 K and 760 mmHg. Calculating the selectivity for a composition containing 15% CO_2 (common for postcombustion gas mixtures), the selectivities are even higher (100−200), indicating that mesostructured PILs are indeed more than suitable candidates for CO_2 capture. Such high selectivities are typically only found in ultramicroporous systems, where molecular sieving phenomena are effective. The fact that such a high selectivity was found in a mesostructured system points again to the special CO_2-philicity of ILs and encourages more research in this direction, especially toward further increasing the still rather low CO_2 capacity.

In summary, a mesoporous poly(ionic liquid) was synthesized, its structure analyzed, and the material screened for its potential in CO_2 separation/utilization. The beneficial effect of the additional specific surface area was proven, while maintaining and even increasing the favorable interactions of the IL with CO_2. The presence of large mesopores can significantly boost the mass transfer through the system, which is beneficial for many applications. The presented pathway can be expanded to other PILs, given the large number of monomer combinations, which could result in even more selective materials with higher capacity and fast uptake kinetics.

■ ASSOCIATED CONTENT

Supporting Information

Materials and methods, analytical data; adsorption data (kinetics and equilibration), and IAST analysis. This material is available free of charge via the Internet at http://pubs.acs.org.

■ AUTHOR INFORMATION

Corresponding Author

*Phone: +49-(0)331-5679569; fax: +49-(0)331-5679502. E-mail: jens.weber@mpikg.mpg.de; jiayin.yuan@mpikg.mpg.de.

Notes

The authors declare no competing financial interest.

■ ACKNOWLEDGMENTS

Financial support from the Max Planck Society is highly acknowledged. We are grateful to Markus Drechsler (University of Bayreuth) for help with Cryo-TEM experiments and to Christoph Weidmann and Bernd Smarsly (JLU Giessen) for technical support regarding the adsorption kinetics.

■ REFERENCES

(1) (a) Anderson, E. B.; Long, T. E. *Polymer* **2010**, *51*, 2447−2454. (b) Yuan, J.; Antonietti, M. *Polymer* **2011**, *52*, 1469−1482. (c) Lu, J.; Yan, F.; Texter, J. *Prog. Polym. Sci.* **2009**, *34*, 431−448. (d) Green, O.; Grubjesic, S.; Lee, S.; Firestone, M. A. *Polym. Rev.* **2009**, *49*, 339−360. (e) Mecerreyes, D. *Prog. Polym. Sci.* **2011**, *36*, 1629−1648.

(2) Yuan, J.; Giordano, C.; Antonietti, M. *Chem. Mater.* **2010**, *22*, 5003−5012.

(3) Pinaud, J.; Vignolle, J.; Gnanou, Y.; Taton, D. *Macromolecules* **2011**, *44*, 1900−1908.

(4) Yoshizawa, M.; Hirao, M.; Ito-Akita, K.; Ohno, H. *J. Mater. Chem.* **2001**, *11*, 1057−1062.

(5) (a) Yuan, J.; Antonietti, M. *Macromolecules* **2011**, *44*, 744−750. (b) Yan, F.; Texter, J. *Chem. Commun.* **2006**, 2696.

(6) (a) Yan, F.; Texter, J. *Angew. Chem., Int. Ed.* **2007**, *119*, 2492−2495. (b) Huang, J.; Tao, C.; An, Q.; Zhang, W.; Wu, Y.; Li, X.; Shen, D.; Li, G. *Chem. Commun.* **2010**, *46*, 967−969. (c) Hu, X.; Huang, J.; Zhang, W.; Li, M.; Tao, G.; Li, G. *Adv. Mater.* **2008**, *20*, 4074−4078. (d) England, D.; Tambe, N.; Texter, J. *ACS Macro Lett.* **2012**, *1*, 310−314. (e) Yan, F.; England, D.; Gu, H.; Texter, J. *ACS Symp. Ser.* **2010**, *1050*, 191−207. (f) Yan, F.; Texter, J. U.S. Patent No. 7,759,401, July 20, 2010.

(7) (a) Schüth, F. *Angew. Chem., Int. Ed.* **2003**, *42*, 3604−3622. (b) Olson, D. A.; Chen, L.; Hillmyer, M. A. *Chem. Mater.* **2008**, *20*, 869−890. (c) Thomas, A. *Angew. Chem., Int. Ed.* **2010**, *49*, 8328−8344.

(8) (a) Thomas, A.; Goettmann, F.; Antonietti, M. *Chem. Mater.* **2008**, *20*, 738−755. (b) Johnson, S. A.; Ollivier, P. J.; Mallouk, T. E. *Science* **1999**, *283*, 963−965. (c) Stein, A.; Wang, Z.; Fierke, M. *Adv. Mater.* **2009**, *21*, 265−293.
(9) Wilke, A.; Weber, J. *Macromol. Rapid Commun.* **2012**, *33*, 785−790.
(10) Marcilla, R.; Blazquez, J. A.; Fernandez, R.; Grande, H.; Pomposo, J. A.; Mecerreyes, D. *Macromol. Chem. Phys.* **2005**, *206*, 299−304.
(11) Gor, G. Y.; Thommes, M.; Cychosz, K. A.; Neimark, A. V. *Carbon* **2012**, *50*, 1583−1590.
(12) Mascotto, S.; Wallacher, D.; Kuschel, A.; Polarz, S.; Zickler, G. A.; Timmann, A.; Smarsly, B. M. *Langmuir* **2010**, *26*, 6583−6592.
(13) Weber, J.; Bergström, L. *Langmuir* **2010**, *26*, 10158−10164.
(14) (a) Tang, J.; Shen, Y.; Radosz, M.; Sun, W. *Ind. Eng. Chem. Res.* **2009**, *48*, 9113−9118. (b) Supasitmongkol, S.; Styring, P. *Energy Environ. Sci.* **2010**, *3*, 1961−1972.
(15) Ostermann, R.; Cravillon, J.; Weidmann, C.; Wiebcke, M.; Smarsly, B. M. *Chem. Commun.* **2010**, *47*, 442−444.
(16) Dawson, R.; Adams, D. J.; Cooper, A. I. *Chem. Sci.* **2011**, *2*, 1173.
(17) Sumida, K.; Rogow, D. L.; Mason, J. A.; McDonald, T. M.; Bloch, E. D.; Herm, Z. R.; Bae, T.-H.; Long, J. R. *Chem. Rev.* **2011**, *112*, 724−781.